Exploring Correlations Between Spatially Heterogeneous Dynamics and Clogging Behavior in a Quasi-2D Granular Silo

by

Giselle Dencker

A thesis submitted to the Department of Physics
in partial fulfillment of the
requirements for the Degree of
Bachelor of Arts in Physics

May 25, 2025

Approved by

Kerstin Nordstrom, Associate Professor,
Department of Physics and Astronomy, Mount Holyoke College
Alexi Arango, Associate Professor,
Department of Physics and Astronomy, Mount Holyoke College
Timothy Farnham, Associate Professor,
Department of Environmental Studies, Mount Holyoke College

ABSTRACT

Jamming is a phenomenon in granular systems that is similar to a thermodynamic phase transition, like freezing. With jamming, a system shifts from liquid-like behavior to solid-like behavior. In phase transitions other features are observed, such as increased fluctuations near the transition point. In jamming transitions, this has been observed as spatially heterogeneous dynamics (SHDs) increasing near the transition [24, 32].

In this work, we investigate whether SHDs occur in granular systems approaching the clogging transition, a transition distinct from jamming. We apply techniques to measure SHDs successfully implemented for jammed systems, such as strings, χ_4, and grain boundaries [32, 36]. Due to the localized nature of clogging, we have focused our are of interest on the more immediate are around the aperture of a system.

We examined experimental data collected by Harada (MHC '18) in quasi 2-D granular silos. With this data we used tracking code that implements the Crocker-Grier method [18, 38], to identify and track particles from frame to frame. With this position data, we are able to identify the crystallinity of the packing throughout our systems. Our goal was to find specially heterogenous dynamics in these systems by finding the amount of disorder in the particle packing of these systems. In addition to this, we compared the trends in the amount of disorder of systems that clogged and systems that did not clog, as well as systems with and without obstacles. We found that an overall higher level of disorder in a system could be correlated to a larger amount of mobility in the system, similar to granular temperature [18].

ACKNOWLEDGMENTS

While I have greatly enjoyed my time as a physics student at Mount Holyoke, it would be a lie to say that it was not difficult. I can truly say that being able to spend the past two years working in Nordstrom Lab has helped me so much. It has given me the opportunity to push myself and do more than just the required work load of this major. If I were not in the lab, I probably would have spent my last year of college fully removed from the Physics department, as I had shifted my priorities to finish the requirements of my Environmental Studies major. While I had not planned on doing a thesis when I joined the lab, doing so has allowed me to push myself and accomplish something I didn't think possible a couple of years ago. While I have learned many valuable technical skills through this process, I have also become a stronger and more competent researcher, scientist, and overall a more confident person. While I do not think continuing a career in academia resonates with me, knowing I was able to push myself in a new way–a way I will probably not get to do again–is something that I will always be grateful for.

There are many people who have made this possible. First, Kerstin Nordstrom, my research advisor, has been endlessly patient with me as I stumbled through this process. Kerstin created an environment that helped me succeed despite not always believing myself to be capable of doing so. My advisors Alexi Arango and Tim Farnham have helped me navigate my two majors along with always checking in to make sure I was also doing well outside of my academics. Lori McCabe, who has spent countless hours debugging code with me, supporting me, taking me for coffee runs during the summer, and always being someone for me to talk to in the lab. I have had many wonderful and supportive lab mates in my time in Nordstrom Lab as well. This past year, my lab mate Zeyu Zhao has been a constant source of joy (and candy) while I worked on my thesis. Outside of the lab, I have had endless amounts of support from my mom and dad, along with constant (only partially annoying) check-ins from my brother.

I have been surrounded by constant love and support from my friends. Setareh Greenwood, my roommate even if we no longer share a room, has always been my shoulder to cry on when the stress has become unbearable. Georgia Camacho has consistently had snacks for me, especially when I am on the verge of tears. My partner, Jeff Black, always reminds me that everything is in fact not hopeless, and that things will eventually be okay. I would also like to thank Molly Rogan, who understands the inner workings of my brain with little to no explanation; Sydney Driskell, one of my best friends since my first week at Mount Holyoke; Abby Brown, my most consistent breakfast companion; Gillian Tomlinson, for always making my coffee with love and never malice; Sophie Pecis, for

always backing me up, especially when I want to complain; Glynnis Goff, for firm hugs and always letting me lean on her when I need to; and Devin Keith, who listened to me practice my senior symposium talk countless times, and who constantly affirms me when I am at my most anxious.

Last but certainly not least, I want to thank Jamie Ambrosina. Jamie passed October 2nd, 2023. Though he has not been here while I have worked on this thesis, he has never been far from my mind, especially during the long hours spent alone in the lab.

As much effort as I have put into my thesis, my loved ones have put infinitely more effort into caring for me. This thesis would not have happened without them, and for that I am eternally grateful.

TABLE OF CONTENTS

LIST OF FIGURES

1 INTRODUCTION

1.1. Granular Materials

A granular material is a large group of macroscopic particles. From 10^1 particles, like a pile of rocks, to 10^{20} particles like sand in a dune field. Granular materials are distinct from other states of matter due to their ability to behave in either a liquid or solid manner [1, 2]. A familiar example of this is beach sand. When densely packed, you can easily walk across it like a solid. This same sand could also be poured into and take the shape of your chosen container like a liquid. This behavior, among other behaviors unique to granular materials, can be seen in many other situations and have practical applications in agricultural, construction, and pharmaceutical industries. These three industries all depend on being able to control the movement of granular materials. Grains and soil are examples of granular materials and are important examples in the agricultural industry. Pills and powders are examples of granular materials in the pharmaceutical industry. In construction, sand is used in concrete and as a feedstock for steel. Granular flow is also a broad topic of research in geology, for example, erosion, landslides, and tectonic movements. Most of our planet's landscapes are composed of soft matter and because of this, the movements of the landscape are based on collective events [3].

A hopper is a container used to hold grains with a funnel at the base for grains to exit through as seen in Figure 1.1. The difference between a hopper and a silo is that a silo has a flat bottom with an aperture, which is the opening the particles are able to leave out of, while a hopper typically has a more funnel shaped bottom. Hoppers are

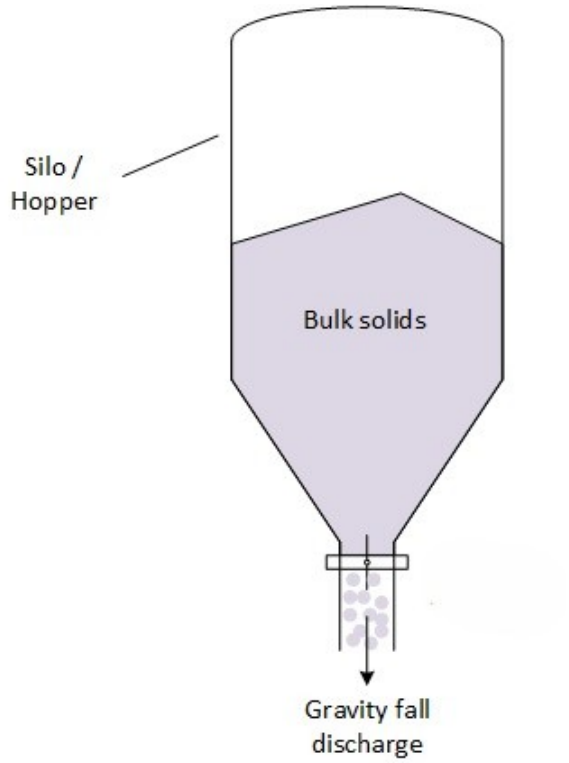

Figure 1.1: Illustration of a hopper from [5].

also commonly called silos, and even though they are different, the terms can be used interchangeably. The flow geometry of a silo has larger scale applications due to how it resembles industrial grain silos, and it is also the flow geometry used in our experiment. These set-ups are useful to collect information about the behavior of granular systems, such as flowing and clogging. Hoppers are widely used for material transport. Hoppers can also be used to develop and test solutions for clogging in full-scale grain silos, along with helping to gain an overall idea of how gravity driven granular materials behave [4]. Simplified grain silos are often used in experiments to learn about clogging behavior and granular flow.

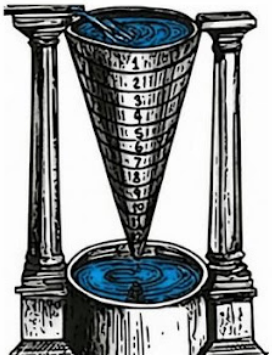

(a) A water clock, the shape and numbering account for the change in volume [7].

(b) A sand timer, also refered to as an hourglass. The mass flow rate is consistent regardless of the amount of sand left [8].

Figure 1.2: Water Clocks and Hourglasses

Granular flow from a silo is quantitatively different from liquid flow. In a liquid the main driver of flow is hydrostatic pressure near the exit aperture. As the liquid flows out, this pressure decreases. Thus, the mass flow rate decreases as the container empties. An example of this is a water clock which was commonly used in Ancient Greece, China, and Babylon, shown in Figure 1.2(a). One version of a water clock is a cone-shaped vessel with different markings to represent each hour. The shape is important because the mass flow rate will decrease as the water flows out, due to the rate of the water flowing out will decrease as the outlet pressure is reduced over time [6, 7].

In contrast to liquid flow, a granular system's mass flow rate does not depend on filling height. This property is used to make sand timers, like you would find in board games, Figure 1.2(b). The mass flow rate and the clogging probability are most affected by the size of the container and the size of the aperture in relation to the diameter of the particles

being used [9, 10]. The mass flow rate is usually described by the emperical Beverloo equation, Equation 1.1 [11].

$$W = C\rho_b\sqrt{g}(D_0 - kR)^\alpha \tag{1.1}$$

W is the average mass discharge rate, C is the discharge coefficent and can depend on friction coefficent of the system. The shape coefficient, k, is specifically based on the shape of the particles in the system. ρ_b is the bulk mass density, g is the acceleration of gravity, D is the diameter of the outlet, R is the particle diameter, and α is a dimensional coefficient which depends on the shape of the aperture. For our experiments we use $\alpha = 3/2$. Filling height and pressure are not aspects of this equation, the key relationship is between D and R. When D/R is less than 5 clogging is likely, though the flow is still o follow the Beverloo equation [9].

1.2. Jamming

Jamming is a non-localized behavior that occurs throughout an entire system. It is a universal behavior in granular materials, as all granular systems have the potential to jam. It describes the shift from particles being able to move throughout a system coming to a standstill [12]. Weeks *et al.* describes a jammed material as an "amorphous solid" or a meterial that is structurally disordered and has a yield stress [2]. A material that possesses a yield stress can elastically deform under low amounts of stress, and irreversibly deforms (yields) under high stress. An example of this is toothpaste, which can maintain its shape on a toothbrush until it is vigorously sheared by contact with our teeth.

As mentioned previously, there are many types of granular materials, and jamming is a way to compare this behavior that is exhibited by different granular systems. This can be due to many factors; three primary factors are load, temperature, and density, as seen in Figure 1.3(a) [13]. Density refers to packing density, or how close the individual particles are to each other in a given volume. Density is equal to the volume of the particles in a system divided by the total volume. Packing density is often shown with ϕ, as seen in Figure 1.4. For example, random closely packed 3D systems generally have a packing density of about 64% [14], random closely packed 2D system have a packing density of about 84%, and 2D hexagonal closely packed systems has a packing density of about 91% [15]. Load refers to stresses (forces) driving the granular system, the driving force of a system is commonly gravity. From thermodynamics, one definition of temperature is the microscopic energy per molecule. The more random motion there is in a system the higher the temperature. The granular research community has defined a similar quantity for grains as granular temperature. Granular temperature is the average kinetic energy associated with the random motions of the grains in a system. This motion could be from random bumping between neighboring particles and can be made more significant by external forces such as vibration or gas-fluidization [16].

Jamming has also been studied as an analogy to the molecular glass transition. The glass transition is when a disordered system becomes so viscous that it is unable to move, and the solid state is freezed in a disordered liquid-like arrangement. Granular systems have been used to try to gain a better understanding of glass systems, as glassy systems can not be directly visualized. This is because the molecules are too small to see, on the order of 0.2nm to 20nm, and optical microscopy has a resolution limit of 200nm.

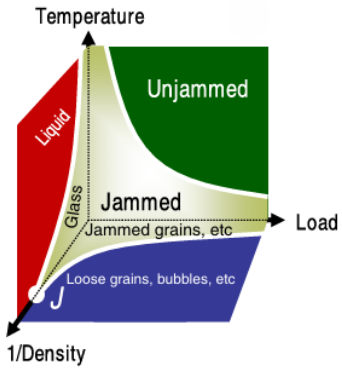

(a) Phase diagram showing how the probability of jamming is effected by density, load, and granular temperature [13].

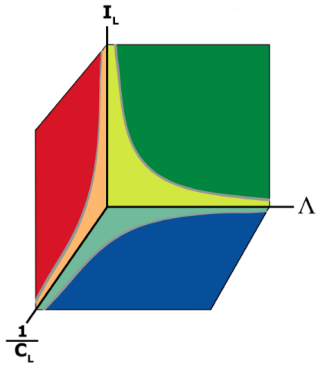

(b) Phase diagram showing how compatible load ($\frac{1}{C_L}$), length scale (Λ), and incompatible load (I_L) increase or decrease the chance of clogging [17].

Figure 1.3: Comparing clogging and jamming.

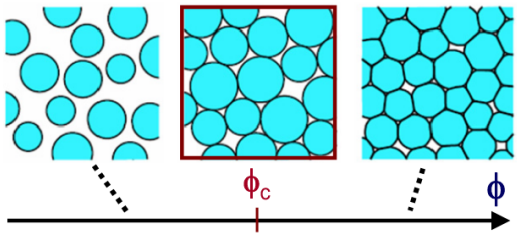

Figure 1.4: This figure from Van Hecke (2010) shows how packing density ϕ effects soft frictionless particles below, at, and above the critical density ϕ_c. Below the critical density the particles have no contacts, at the critical density the system is more ridged and the particles are just touching, and then above the critical density we see a jammed system with particles firmly touching. Due to the fact that these are soft particles, they are also deforming [13].

1.2.1 Jamming vs. Clogging

Jamming and clogging in a system can be visually similar, since in both cases the system changes behavior and stops moving. A key difference between clogging and jamming is the fact that clogging is a localized behavior, usually occurring at a bottleneck. A bottleneck refers to a smaller passage where particles are being funneled; for example, a large room of people trying to leave through one small door. Depending on the density, speed, and force of the motion of people, they will clog at the door leading to a standstill unless something changes, for example, another door opening or people being moved around. Similar to pouring grain through a funnel, there is a chance the funnel will clog. This is defined as the clogging probability. This clog can then be broken up by disturbing the grains which will grant room for movement.

This variation in clogging probabilities is either increased or decreased based on experimental conditions and can be manipulated accordingly [18–20]. For clogging we look at compatible load, length scale, and incompatible load, Figure 1.3(b). Compatible load, comparable to load for jamming, refers to the driving force in the system, in our case this is gravity. Length scale refers to the comparison of particle size to outlet size [17]. In our research, and a majority of the literature, the diameter of the particles are used as a unit for normalization throughout the experimentation set-up, as mentioned in Section 1.2 systems tend to clog when $D/R < 5$. Incompatible load refers to a force that could unclog a system, for example vibrating the system to dislodge particles. Incompatible load is analogous to granular temperature for jamming. In our experiments incompatible load is the addition of an obstacle which introduces randomness in both motion and structure [18].

2 BACKGROUND

2.1. Spatially Heterogeneous Dynamics

Spatially heterogeneous dynamics (SHD), refers to the differing behavior of particle movement throughout a system, specifically when multiple speeds can be observed across a system, with no apparent organization. This behavior was originally seen leading up to glass transitions [21, 22]. Further research and experimentation showed that SHD is also present in granular systems leading up to the jamming transition [23, 24]. These behaviors can be looked at throughout a system to gain a better understanding of jamming. For both glassy and granular systems, an increase in SHD as these systems approach the glass or jamming transition has been observed. To know if there is an increase in SHD, one must find a way to recognize and calculate the amount of area they are taking up in a system [25–31].

2.2. Strings

One way to find and categorize SHD is strings. As the name implies, strings are groups of particles that move through a system. More specifically, a string refers to particles that are directly replacing the position of a neighboring particle within a set time. This creates behavior similar to a conga line on a crowded dance floor. Finding these strings and calculating the area they take up in a system over time can help determine if there is an increase or decrease in SHD leading up to a transition in behavior [32, 33].

Keys *et al.* [24] looked at the prevalence of strings leading up to the jamming transition. They used data from an experiment by Abate *et al.* [23, 32]. The system has an equal

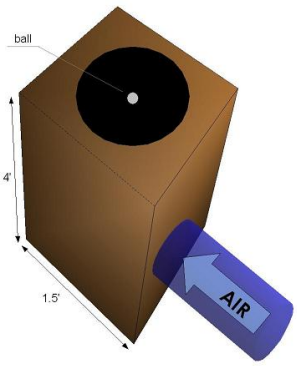

(a) Scamatic of the experiment. The particles used in this system were steel spheres of two sizes, 0.318 and 0.397 cm.

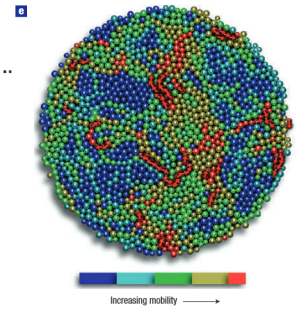

(b) The clusters of strings are colored based on their speed during a 12s period . The red particles represent the particles with the most mobility, and the red particles with arrow vectors are strings [24].

Figure 2.1: Experimental set up from [32] and the analysis done by [24].

amount of two different sizes of steel beads, 0.318 cm and 0.397 cm. While this experiment uses two different sized beads they were not actively looking at what effects it might have on the system. The beads were confined in a horizontal circular system and excited with upward airflow, like an air hockey table as seen in Figure 2.1(a). They then tracked the particles, their neighbors, and velocities to map out strings in the system, as seen in Figure 2.1(b). They found that there was a positive correlation between the presence of strings and the density of the sytem [24].

2.3. Four-point Susceptibility

Four-point susceptibility, also known as χ_4, is another way to measure heterogeneous behavior in a system. χ_4 is not a direct measurement of SHD, but it is correlated. χ_4 is a way of seeing the amount of mobility in a system, which is related to SHD [24, 32].

χ_4 requires a few steps to define. At the core is a quantity called the self-overlap parameter, w. In brief, we measure the position of one particle, and ask if it overlaps "itself" in a subsequent frame. If it does overlap, it is given the value of 1; if it has moved more than one radius from its initial position, then the value is set to 0.

$$w = (|r_i - r_j|) = \begin{cases} 1: & \text{if } |r_1 - r_2| < a_0 \\ 0: & \text{otherwise} \end{cases} \tag{2.1}$$

a_0 is the distance a particle can move between being in its original position and being fully in the position of a neighboring particle. a_0 is typically set to $\langle R \rangle$, which is the average bead radius of the system, though there are inherent limitations in any choice, especially if the motion is highly variable. Next a parameter, Q, is calculated in Equation 2.2. $Q(t, \tau)$ is the fraction of particles that have stayed within a distance of a_0 from their original position at time t over the time interval τ. As the particles in a system move around from their initial position, the area fractions affect how quickly $Q(t, \tau))$ decays. The area fraction is similar to the packing density. The difference being that the area fraction is the space in a specified area that is taken up by the particles, while the packing density refers to the mass in a certain volume. $Q(t, \tau)$ goes to zero when a particle has completely moved away from its original position. This measurement can be taken at multiple times and averaged to get the time averaged order parameter, $Q(\tau)$.

$$Q(t, \tau) = \frac{1}{N^2} \sum_{i=1}^{N} \sum_{j=1}^{N} w(|r_i(t) - r_j(t + \tau)|) \tag{2.2}$$

(i=j) a particle overlaps with itself

(i$\neq$ j) a particle overlaps with a different particle

As stated previously $Q(\tau)$ refers to the averaged order parameter. τ is the time interval, and t is the time the measurement is taken. N is the number of paticles in the system. r_i and r_j are used to indicate the position of the particle and if it overlapping with itself or another particle, as previously defined in Equation 2.1. $i = j$ means the particle overlaps with itself and $i \neq j$ means the particle is overlapping with another particles position.

How quickly $Q(\tau)$ decays depends on the packing density of the system. If a system is very tightly packed it is more difficult for particles to move from their original positions. In comparison, a less dense system has more freedom to easily move around, leading to $Q(\tau)$ decaying quickly. SHD in time and space will make the individual measurements of Q vary, so to capture the SHD we calculate the variance of Q. The normalized version of this parameter is χ_4, Equation 2.3 [32, 34, 35]. Figure 2.2 shows how χ_4 increases as a system approaches jamming due to an increasing packing density.

$$\chi_4 = N|\langle Q(\tau)^2\rangle - \langle Q(\tau)\rangle^2| \tag{2.3}$$

χ_4 is generally easier to interpret in jammed systems due to the fact that there is some inherent symmetry in them. We can still compare the difference in the height of the χ_4 peak and the location of the delay time peak. Clogging systems are harder to interpret due to the lack of symmetry and their localized nature. This can be observed in the fact that there is a secondary peak, or "shoulder", in the distribution, as shown in Figure 2.3. χ_4 shows the variance of Q, or the heterogeneity of the mobility in a system. Previous reaserch in the Nordstrom Lab has been done looking at χ_4 in clogging systems, and they

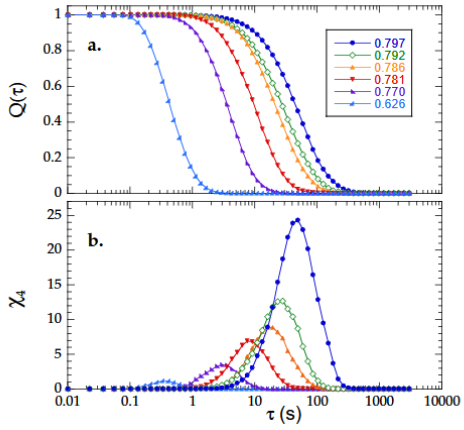

Figure 2.2: This figure is from Abate's 2006 thesis. Figure a shows the overlap order parameter and figure b shows the scaled variance, which is χ_4. The different lines refer to different area packings. The higher the area packing, the longer the system is static [32].

were able to get results and see a trend in behavior, specifically that cooperative motion increases with aperture size, but χ_4 does not tell you where SHD are in a system and the results are difficult to interpret [36].

2.4. Grain Boundaries

Grain boundaries are another way to look at string-like behavior in a granular system. Instead of using χ_4 to characterize strings in a system we can use local packing structures to identify clusters in the system. These clusters have crystalline, or close to crystalline, packing, illustrated in Figure 2.4. This generally means they have the maximum amount of neighbors within a specific distance. These clusters are separated by patches, or generally smaller groups, of particles with non-crystalline (less densely packed) particles. The amount of clusters and the number of particles in these clusters inform us how much space they occupy in the system. With this information, we can calculate the area of the grain

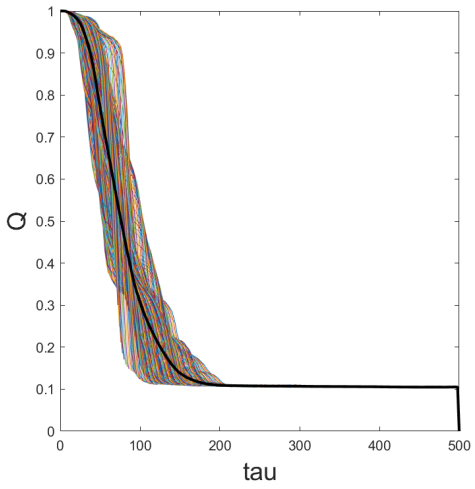

(a) The particles in a system move from 1, overlapping with "itself", to 0, in a new position. The different colored lines indicate different instances of measurements being taken. This graph does not fully decay to zero. This is due to the set-up used in this experiment, Figure 3.1, there are particles in the bottom left and right corners that never move.

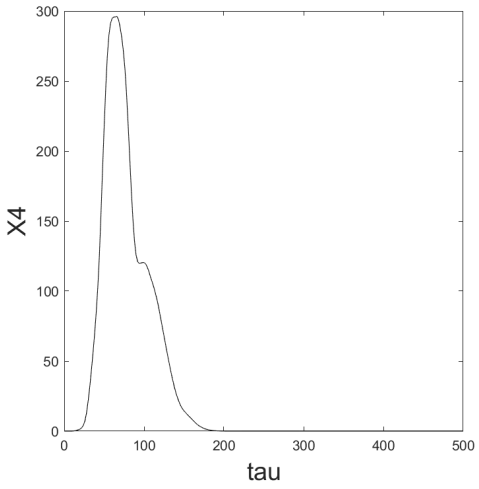

(b) c oorresponding χ_4 graph for the (a) Q distrabution. The shoulder indicates that there are multiple time/length peaks present.

Figure 2.3: Comparision of Q and χ_4 graphs made form the same experiment data. These graphs are from an experiment with a set-up of 4.5D aperture and a 5.5D obstacle which was placed 6D above the aperture.

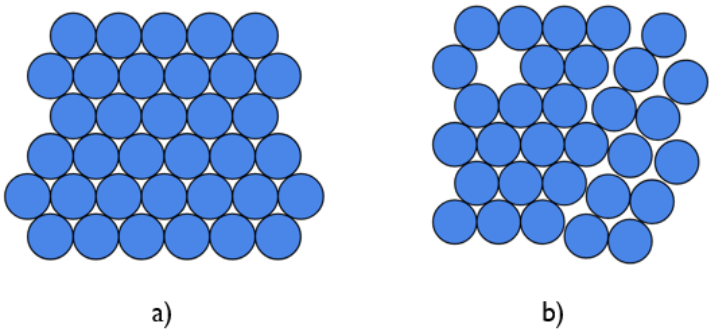

Figure 2.4: a) An example of a crystalline packing, specifically a hexagonal packing structure, commonly known as a "hex" packing. b) An example of non-crystalline packing. Specific types of disorder in packing a dislocations, individual missing particles, and disclinations, which are lines of out of place particles, both of which are shown in figure b).

boundaries in our total system. Grain boundaries are the less tightly packed regions between clusters. Grain boundaries are extremely likely to have strings within them, and there is correlation between an increase in the number of grain boundaries and an increase in SHD [24, 37, 38]. This method was used to observe the effects of having varying concentrations of bidispersed particles in a system in Berardi *et al.* [37]. The particles used in the system were 3 mm and 2 mm chrome spheres. They looked at two concentrations of the smaller particles. The low concentration was when 3% of the total particles were 2 mm, and the high concentration was 10%. They used a rectangular quasi-2D set-up, but unlike our set-up, Figure 3.1, there was no aperture and the system was shaken to create random motion.

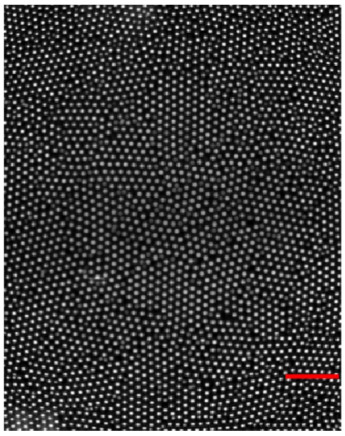

(a) raw image from the experiment. The red line is for scale and is equal to 2 cm [37].

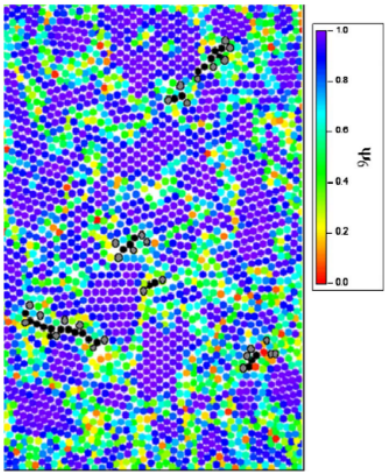

(b) The color bar indicates the packing of the particle. Ψ_6 is how close a particle is to being in a hexagonal packing with purple being a hexagonaly, or near hexagonally, packed particle and red being the furthest away form being considered hexagonally packed. The black dots are particles that are a part of strings [37].

Figure 2.5: These images are from Berardi *et al.*(2010). They are of the particles from an experiment with a higher concentration of smaller particles.

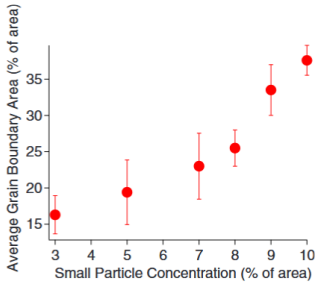

(a) The average percent of area taken up by grain boundaries increases as the small particle concentration increases.

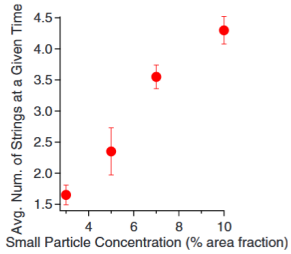

(b) The average number of strings in a system increases as the small particle concentration increases.

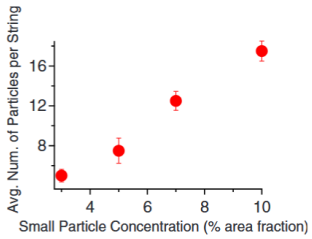

(c) The average number of particles in a string increases as the small particle concentration increase.

Figure 2.6: Results from Berardi *et al.*, showing the effects of increasing small particle concentration in a system [37].

Berardi *et al.* identified grain boundaries in the system, based on the packing structure, and strings within those grain boundaries. They found that increasing the concentration of smaller particles leads to an increase in the total area the grain boundaries occupies in the system, the number of strings present in the system, and the number of particles in those strings as seen in Figure 2.6. These graphs show that increasing disorder in a system leads to an increase in SHD. This due to the systems having a higher concentration of small particles which leads to an increase of behaviors, like strings and grain boundries, that indicate SHD.

3 EXPERIMENTAL WORK

The data referenced throughout this thesis was taken by Harada (MHC '18), and some analysis results were published in 2022 [18]. This chapter details the methods and results from that paper, along with changes we have done to the code, specifically to improve the featuring and tracking of the videos.

3.1. Experiment Background

Data on flow and clogging probability was collected using a quasi-2D granular silo to see how the introduction of an obstacle impacts the system. The silo is made of transparent acrylic walls, with a gap created between the sheets of acrylic and the exit structures made of a teflon insert, as seen in Figure 3.1. The particles used in the experiment are acrylic spheres with 3.160 ± 0.002 mm (Engineering labs, Oakland, NJ). A teflon circle is used as an obstacle by fixing it to the acrylic wall with tape. The teflon, acrylic, and the T-slot aluminium that creates the frame are all from McMaster-Carr. These teflon circles were cut using a laser cutter in the Fimbel Maker and Inovation Lab at Mount Holyoke College. The plug for the aperture was 3D printed with PLA filament. Five obstacles of various sizes were used: 3D, 5.5D, 10D, 17D, and 30D where D indicates one particle diameter. Particles are added into the silo until mostly filled, and then a video is taken as the plug in the base of the silo is removed to release the particles. The recording is stopped when the silo fully clogs or all the particles exit the silo. The camera used is a Phantom V1611 camera (Vision Research) to film up to 1000 frames per second at a resolution of 1280 $\times$ 800 pixels. Experiments were carried out with each obstacle size at five heights from

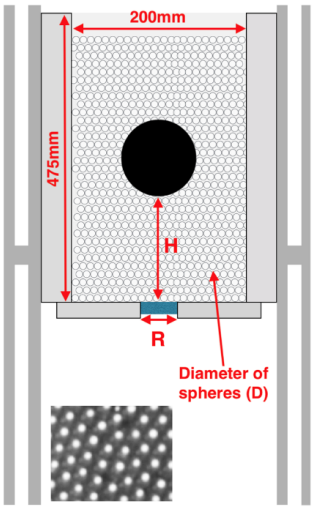

Figure 3.1: Diagram of experimental set-up from Harada, 2022. This diagram is not to scale, refer to the measurements in red. R is the width of the aperture and H is the height from the bottom of the obstacle to the top of the aperture. Both of these measurements are in units of the diameter of the particles, D.

the aperture: 3D, 6D, 8D, 10D and 15D. Each experimental set-up had a minimum of five trials in order to estimate the clogging probability based on the number of those trials that clogged. These experiment sets were taken with 5D sized aperture, and then again with a 4.5D sized aperture. Results from the 5D trials are published in [18], the results from the 4.5D trials are unpublished. As mentioned previously, when the aperture gets to around 5-6D there is a transition in the clogging behavior. Around that range the clogging probability is significantly increased, and the system is more likely than not to clog. The goal in the Harada paper was to see the effects of an obstacle on the clogging probability, so picking these aperture sizes helped observe these effects in a systems that otherwise had a high clogging probability without the obstacle [18].

3.2. Featuring and Tracking Code

The tracking code implements the Crocker-Grier tracking method [39]. This code does two main things, featuring and tracking. Featuring refers to code recognizing the individual particles in all the frames from an experiment video. After a bandpassing step to filter out noise, candidate particles are first identified as bright spots. The bright spots that are particles should fit well to a 2D Gaussian intensity pattern. To identify particles we set variables with what to look for, specifically ranges for particle size, and brightness. Then the particles are given a unique integer particle ID and are tracked from frame to frame by setting a range for the amount of movement we expect from the particles, based on frame rate.

This code was used in the Harada paper, though it got a significant amount of false positives at the time which were managed by doing post-processing filtering. False positives refers to particles that did not exisit but were identified during the featuring portion of the code. These were mainly due to uneven lighting of the experiments. We reduced the amount of false positives by changing the image processing that happened prior to the featuring step in the code, and then added additional filters while featuring to remove more false positives which also had the benefit of increasing computational efficiency.

Changes made to the code to reduce false positives include: fine-tuning variable choices for *memory*, *particle size*, *max movement distance*, filters to the frames of the video including *binarization* and *gradient* prior to bandpassing and then removing particles below a certian size or brightness, as shown in in Figure 3.2(a-d). *Memory* refers to how many frames the code should keep looking for a particle if it loses it, before "forgetting" it. *Binarization* and *gradient* are both image filters that helped make the brightness

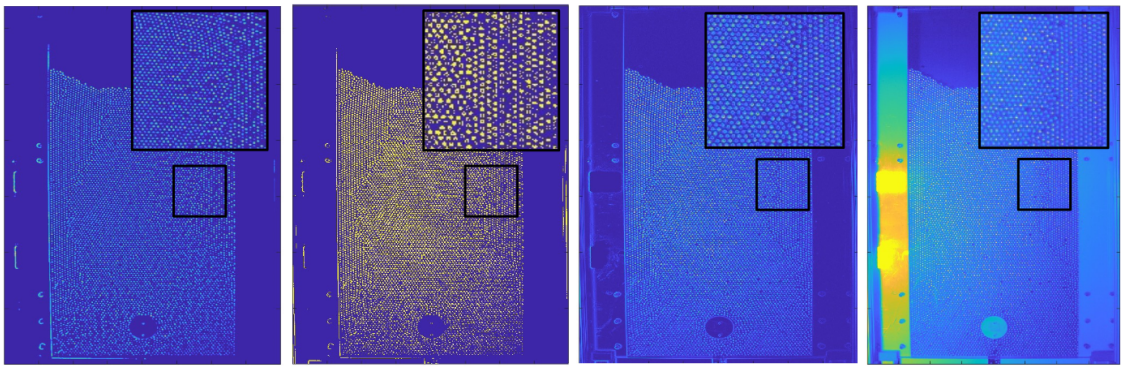

a) b) c) d)

Figure 3.2: Images showing the filtering steps used durring the featuring portion of the feturing and tracking code. a) Gradient, b) Binarize, C) Bandpassing, D) Removing particles. Once all the steps are completed the brightness of the particles is more even. These steps made the particle brightness more consistent but they did increse some of the inconsistancies on the boundry of the system.

of the particles more consistant. These steps greatly reduced the amount of false positives along with a filtering code that cut off the sides of the videos where the walls of the silo were visible. This was due to false positives appearing on the walls of the system creating due to the lighting of the videos and the contrast of the white teflon on black backgrounds.

While we were able to remove most of the false positives in the system, we now lose some particles, for the very similar reason of lighting inconsistencies making it difficult to see some particles in darker areas of the experiment videos. While not perfect, this is not a major concern of ours as we are generally only losing around 10 particles in a system that has almost 10,000 particles on average. This is on par with, or even much better than similar experimental work [19]. A member of the Nordstrom Lab, Zeyu Zhao (MHC '2027), has worked to further improve this featuring and tracking code, and has gotten it to be almost perfect.

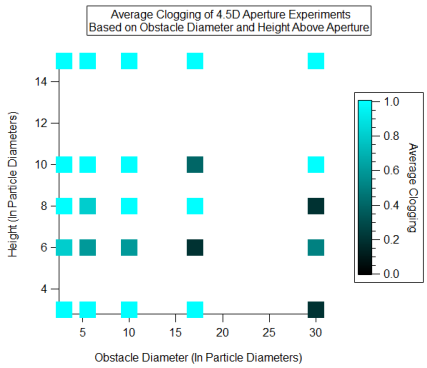

(a) The clogging averages for the experiment set-up with the 4.5D aperture. Overall, a majority of the experiments clogged.

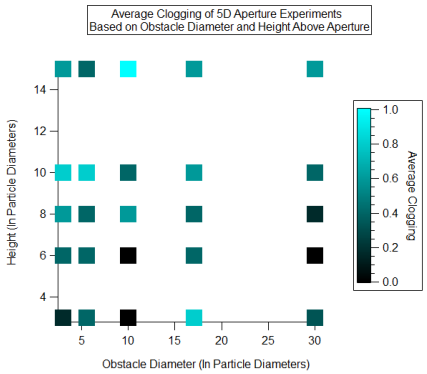

(b) The clogging averages for the experiment set-up with the 5D aperture.

Figure 3.3: Phase maps showing the clogging averages for experiments with 4.5D and 5D apertures. Different experiment set-ups are based on the size of the obstacle used and the distance from the bottom of the obstacle to the top of the aperture. Clogging data was gathered by looking through each video. 1 indicates that all the trials in that experiment set clogged and 0 indicates that none of the trials in that experiment set clogged.

3.3. Obstacles Effects on Clogging

Outlet size has been shown to affect the probability of clogging in papers besides the Hadara paper [40, 41]. Harada found that with an aperture of size 5D and no obstacle there is a clogging probability of 73%. Overall for the 5D aperture, clogging was reduced with the presence of an obstacle. With the 5D aperture obstacle experiments we got a range of 0% to 80% among all experiment set-ups with a total average clogging probability of 44.5% across all trials. These experiments with lower clogging probability generally have a set-up with obstacles that are larger and closer to the exit aperture, as seen in Figure 3.3(b) [18].

As previously discussed, there is a higher chance of clogging in experiments with a smaller aperture. This is seen in the comparison between the experiments with the 4.5D

aperture to the experiments with the 5D aperture. In the 4.5D set-up there is a clogging probability range of 20% to 100% throughout all experimental configurations with a 4.5D aperture and a total average clogging probability of 80.9% across experiment trials. Out of the 25 different experiment set-ups done with a 4.5D sized aperture 16 of them clogged in all 5 trials, for 100% clogging probability. While the addition of an obstacle is able to reduce the clogging probability of a system, the comparison between the 4.5D and 5D experiments with an obstacle show that the aperture size still has significant influence on the clogging probability of these systems.

3.4. Obstacles Effect on Particle Flow

Another key effect of the introduction of an obstacle to these systems is how it affects the flow of the system. Harada analyzed the flow in a system with a 5D sized aperture by looking at the velocity of the particles based on the amount they moved frame to frame. The results from the Harada paper showed that a larger obstacle size lead to higher horizontal granular temperature and a higher granular temperature by the exit region, as seen in Figure 3.4. The exit region refers to the area of the system by the aperture [18].

When analyzing the 4.5D sized aperture data we looked at similar metrics but in a different way. We looked at the overall average velocity magnitude (V_{mag}), velocity in the x-direction (V_x), and V_x standard deviation for every particle in a system throughout the entire experiment run. V_x can show us if there are any distinctive flow patterns, V_{mag} helps us understand the mobility of the system, and the standard deviation of V_x shows us the horizontal granular temperature of the system. Granular temperature, discussed in Section 1.2, is quantitatively described as the standard deviation of V_x. Horizontal granular temperature can also be described by Equation 3.1 [41]. Horizontal granular temperture

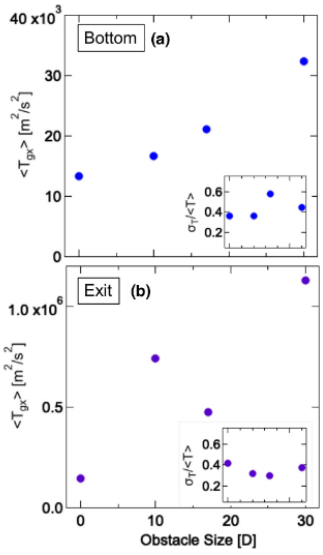

Figure 3.4: Graphs from Harada *et al.* a) Horizontal temperature in the bottom of the silo compared to obstacle size. b) Granular temperature by the exit of the silo compared to obstacle size. To look at the exit we reduce the height and width of the area we are looking at, while when looking at the bottom are we just reduce the height of the area [18].

helps us get an overall idea of the random motion in the x-direction, which gives us a clear idea of mobility in the system.

$$T_{gx} \sim \langle \delta V_x^2 \rangle = \langle (V_x - \langle V_x \rangle)^2 \rangle \tag{3.1}$$

The Figures 3.5, 3.6(a), and 3.6(b) show the averages of these averages for each different experimental set-up. We found for the 4.5D aperture experiments there was no preference towards the negative or positive x-direction, as seen in Figure 3.5. When comparing the 4.5D clogging graph, Figure 3.3(a), and the 4.5D average V_{mag}, Figure 3.6(a) we can see that the experimental set-ups with larger obstacles placed closer to the apature, the bottom right corner of the graph, have higher an overall V_{mag} and lower clogging probability. This countinues with a comparision to the V_x standard deviation graph, Figure 3.6(b), where those same experiments also have an overall higher Vx standard deviation. Inline with Harada's 5D experiments, we see a higher fluidity with the introduction of an obstacle.

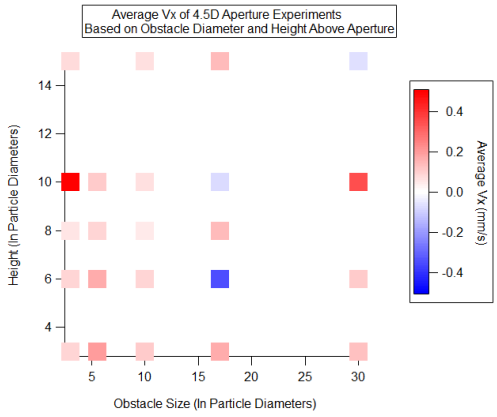

Figure 3.5: Average velocity in the x-direction across an experiment set compared to obstacle size and placement. The data that makes up the average is the total average velocity in the x-direction from the individual videos in the experiment sets.

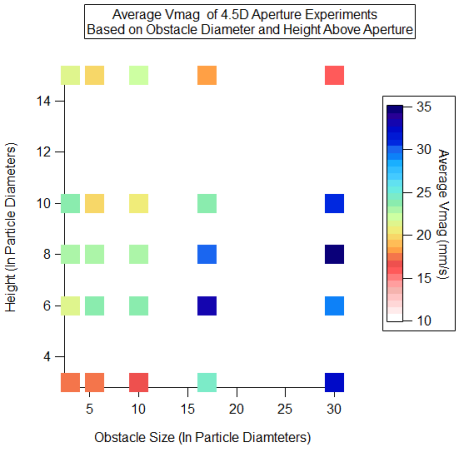

(a) The average magnitude of the velocity, across an experiment set. The data that makes up the average is the total average magnitude of the velocity from the individual videos in the experiment sets. While the majority of these experiments clog, the addition of the obstacle still lead to an increase in fluidity.

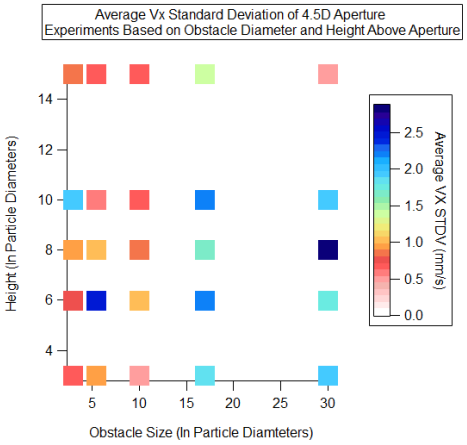

(b) The average standard deviation of V_x across an experiment set compared to obstacle size and placement. The data that makes up these average is the average standard deviation of the velocity in the x-direction from each video with the same experimental set-up.

Figure 3.6: Phase diagrams of 4.5D experiments with varying obstacle size and placement.

4 METHODS

4.1. Particle Tracking

As previously discussed in Section 3.2, the data collected and used by Harada *et al.* was first run through tracking and featuring code. We made edits to this code to more accurately track our particles. This was due to some uneven lighting that caused false positives in addition to losing some particles during tracking. Along with tracking the particles to get position data, we also collect additional data about the experiments such as: the average V_x, the average V_{mag}, the average standard deviation V_x, the number of particles in the first frame, and the total number of particles tracked. We get one value per experiment for each of the previously mentioned averages. Some identified particles are not always correctly identified throughout the entire video. This means there is usually a higher number of identified and tracked particles than the number of particles in our first frame, which should be the total number of particles in the system. This is not a concern of ours as in comparison to the total amount of particles in our system we are misidentifying or losing very few particles. In addition, what we use the position data for in the code discussed in the following section, is not effected by a particle not having the correct particle ID. This is because the code is looking at the positions of the particles in each individual frame rather than a particle's entire path through the system.

4.2. Crystalline Shielding Code

The crystalline shielding code we used was originally created for, a paper by Teich *et al.*, 2021 [19]. The goal of this paper was to investigate local structures in a jammed 2D

macroscopic system under oscillatory shear and compare these results to "rearrangement, memory, and macroscale rheological measurements". This experiment was done with sulfate-coated latex (Invitrogen) particles with a packing density of 14,300 particles/mm^2 for the monodispersed system and 16,500 particles/mm^2 for the bidispersed system. In more straightforward terms, they were aiming to connect structural characteristics to dynamical responses, how a system changes and moves, while under stress. Understanding how systems rearrange under stress would help to predict and manage events; for example landslides are a product of a disordered structure unjamming. Being able to predict and prevent this from happening would be very beneficial for people's safety [19]. They used the code to observe how much the particles towards the center of a cluster, or more "shielded" particles, shifted positions as a system is sheared. They found that more shielded particles stayed closer to their original positions, and therefore had a "memory" of their initial placement.

The shielding code identifies clusters in a granular system by thresholding particles based on the number of neighbors each particle has, and the distance between the particles and their neighbors. We set the distance threshold based off of the $g(r)$ measurements of the systems we are looking at. $g(r)$ is the radial distribution function, and it tells us how predictable the distance from the center of one particle to the center of its closest neighbor is [42]. This is done by finding all the particles within a set distance, r, from the particle being looked at, averaging this for the whole system, normalizing based on the area being looked at and the overall density of the system, and finally repeating for a different r, as seen in Figure 4.1(a).

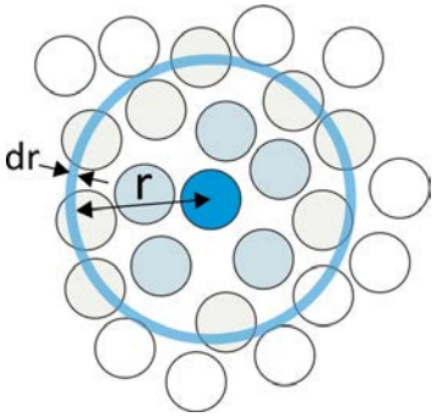

(a) diagram showing how a doughnut with a width of dr is used along with r to look at the distances between a particle and its neighbors using the radial distrabution function [42].

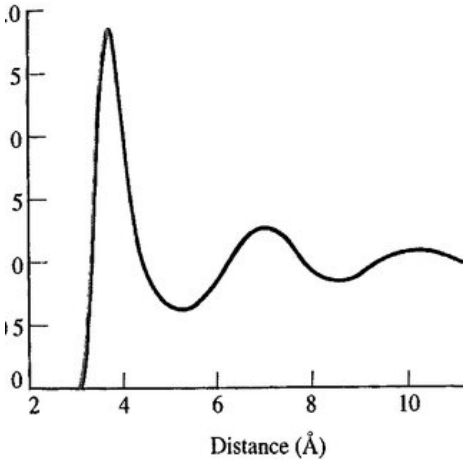

(b) Graph shoing the radial distrabution of liquid argon [43].

Based on the $g(r)$ measurements from our systems, seen in Figure 4.2, we set the distance threshold at 9 to included a majority of what are considered the closest neighbors in the system. If the distance is too far or the particle does not have enough neighbors, the particle will not be counted as part of a cluster. This is done for all the particles in a frame, and then repeated for every frame in a video. In addition to finding clusters, the shielding code is also able to categorize the particles in clusters based on how close they are to the boundary of a cluster, but we did not use this portion of the code.

While χ_4, strings and the method used by Berardi *et al.* to look at grain boundaries are all methods to measure SHD, we ended up focusing on a different approach. Due to large clusters within our system, this "inverse" approach using the shielding code seems more fruitful than measuring grain boundaries directly. We used this code by connecting it from Python to MATLAB, to easily integrate it with our other analysis codes, and running our data sets of particle position data through to get various outputs. This is done by creating

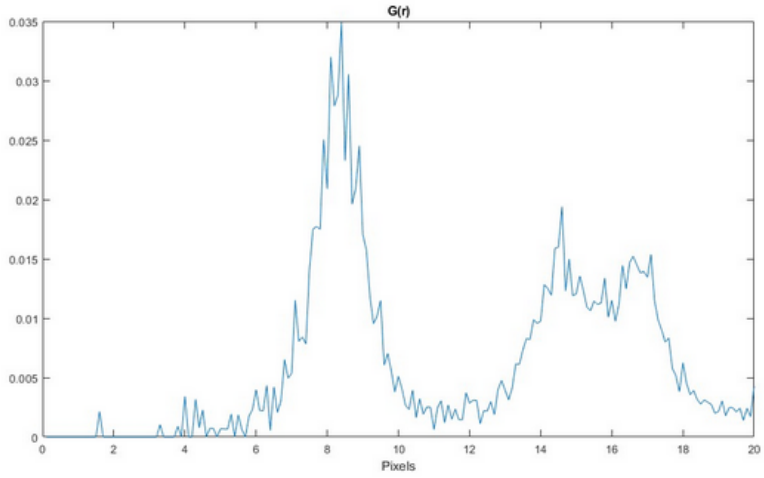

Figure 4.2: $g(r)$ graph with a main peak around 8, meaning a majority of particle's nearest neighbors are within 8 pixels. We use 9 for our thresholding as it includes more particles.

a Python environment for MATLAB use and then calling the shielding code from that environment. From this code we get images of each frame showing the various clusters. These images can be compiled into a video to better observe how the different cluster move and change throughout the experiment. In addition to these images, we can also collect the data of the number of particles included in clusters, or not. This is beneficial as we can observe if there is an increase or decrease in noncrystalline areas where grain boundaries are located.

5 RESULTS

For our results we focused on getting a visual representation of the crystalline and non-crystalline clusters in our system. We were also interested in measuring the amount of area the areas of non-crystalline packing, or disordered packing, occupied and how that changed as the system emptied. Due to time constraints we were unable to run this analysis on all the experiment datasets we have available. We chose two experiments with the same set-up without an obstacle and two more videos with an obstacle. For both sets of two experiments we have one that clogs and one that does not clog. These experiment set-ups were chosen due to the relatively equal chance for a clog to occur based on the estimates from our experiments.

5.1. Crystalline Cluster Videos

Using the shielding code on our data sets gave us two initial outputs. The first is a scatter plot creating a visual representation of the clusters in the system. We get one plot per frame in an experiment, and we are then able to create a video with these scatter plots to see how the areas of crystalline packing and noncrystalline packing visually change over time, as seen in 5.1.

These graphs are interesting to use to observe how the packing changes in different areas while the system flows. In addition they can be used as a sanity check for results discussed in later sections as they give us a visual representation of the amount of disorder to expect in a system.

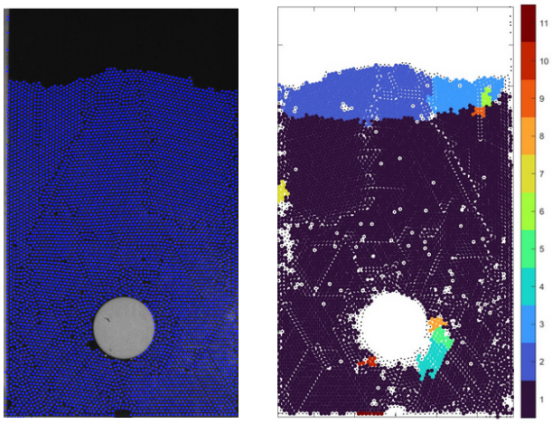

a) b)

Figure 5.1: A frame from a video that was taken by Zeyu Zhao and tracked with her updated version of the tracking and featuring code. a) tracked frame from experiment video. b) same frame run through shielding code. The color bar shows the colors of the different clusters in order of size with 1 being the largest cluster.

5.2. Disordered Area

Using the data that creates the scatter plots and histograms mentioned above, we can find the total number of particles in each frame, along with the number of particles that are not crystalline. With these numbers we can find the percent of the total particles that are non-crystalline, or the percent of total area that is disordered. We created line graphs for various data sets to compare how the percentage of disordered area changes in clogging and non-clogging experiments vs. time. Due to the localized behavior of clogging we wanted to focus in on the aperture. To do this we ran the analysis with the shielding code multiple times with different methods of cropping the data, as seen in Figure 5.2.

5.3. Obstacle

The clogging experiment in these graphs is from an experiment that went a bit longer compared to the clogging experiment without an obstacle. For the most part, it appears that

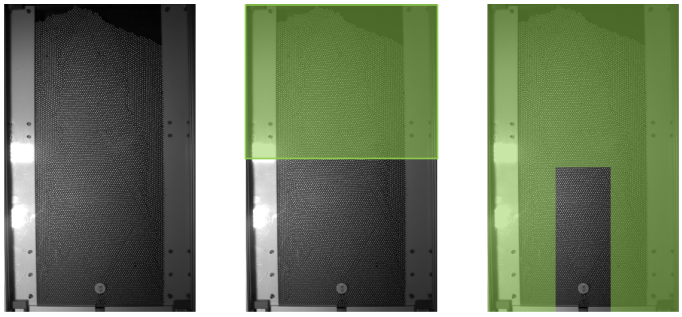

Figure 5.2: Cropping used for shielding code analysis, the green indicates areas of the system not included in the analysis. a) No cropping. b) Half cropped. c) Full cropped.

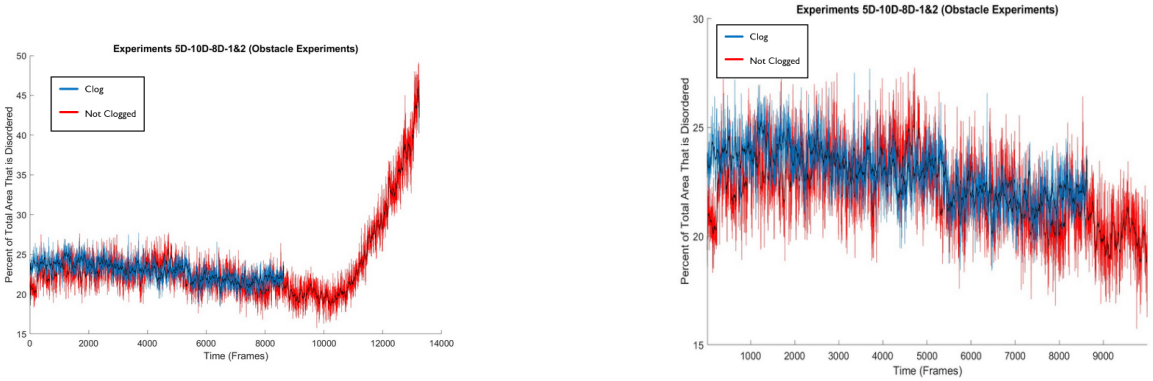

(a) (b)

Figure 5.3: Experiments with a 5D aperture, 10D sized obstacle placed 8D above the aperture, and no cropping done. b) is a zoomed in version of a).

the clogging and non-clogging experiments align pretty consistently, as seen in Figures 5.3, 5.4, and 5.5. The experiments with no obstacle have an overall lower amount of disorder compared to the experiments with obstacles. For example, Figure 5.5(b), which is the fully cropped and zoomed in graph from the obstacle experiments, has a range of disorder around 12% to 22%, while Figure 5.8(b), which is the fully cropped and zoomed in graph from the no obstacle experiments, has a range around 4% to 8%.

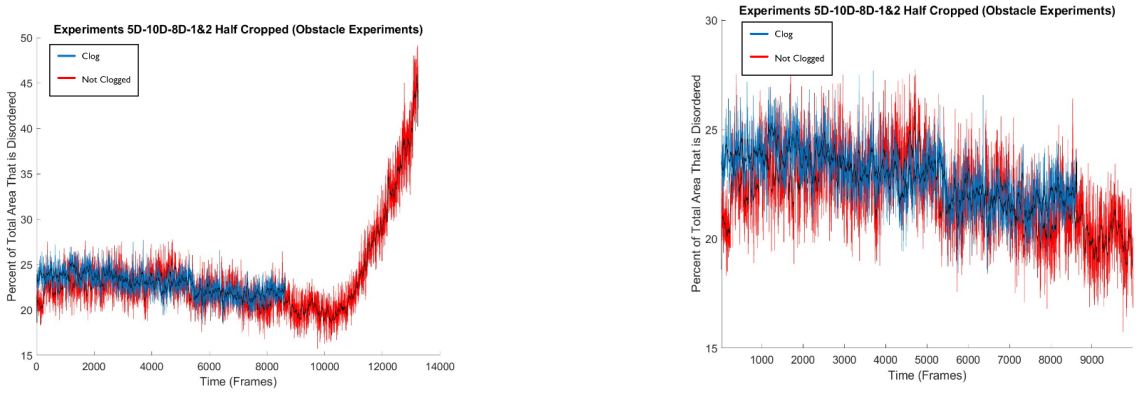

(a) (b)

Figure 5.4: Experiments with a 5D aperture, 10D sized obstacle placed 8D above the aperture, and half cropped. b) is a zoomed in version of a).

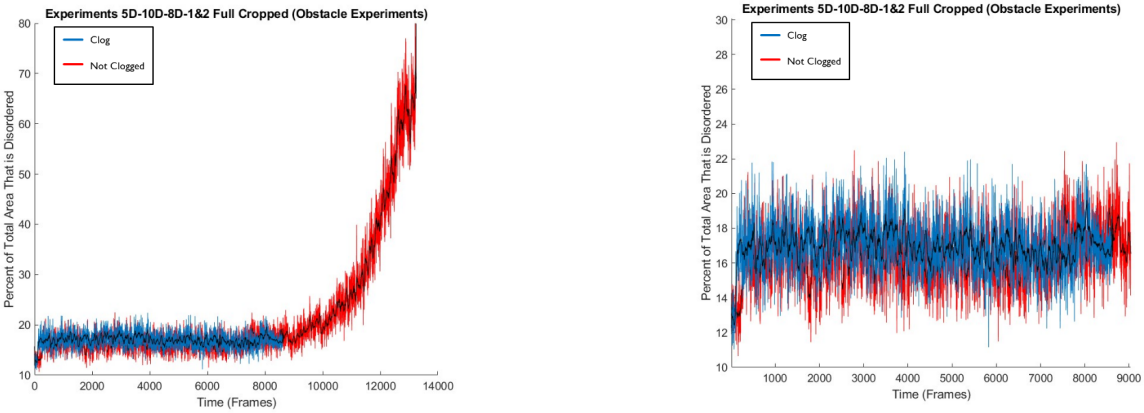

(a) (b)

Figure 5.5: Experiments with a 5D aperture, 10D sized obstacle placed 8D above the aperture, and full cropped done. b) is a zoomed in version of a).

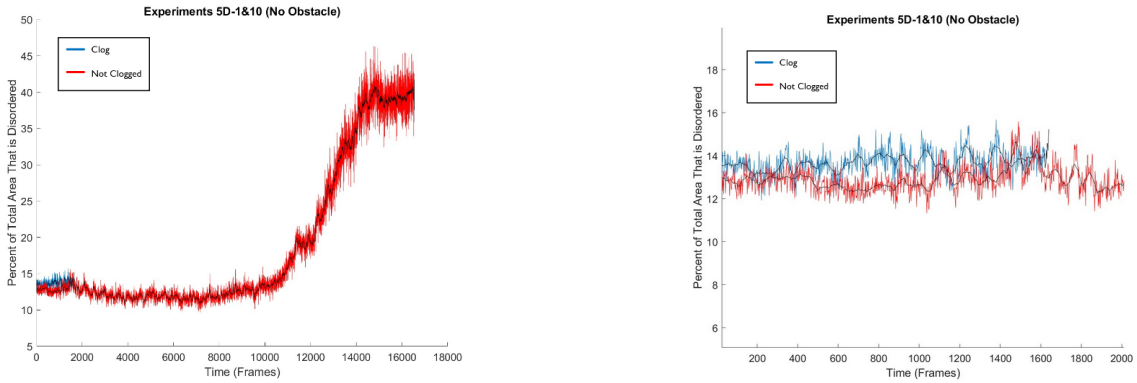

(a) (b)

Figure 5.6: Experiments with a 5D aperture, no obstacle, and no cropping done. b) is a zoomed in version of a).

5.4. No Obstacle

Like the experiments with obstacles, the trend of the clogging and non-clogging graph align well, as seen in Figure 5.6. Though there is notably a higher level of disorder in the clogging experiment when it is half cropped in Figure 5.7. We believe this is due to areas of disorder in the bottom corners of the silo. These corners do not move much, so there would minimal amount of change to the packing in these areas. They would be a more prominent majority of the system when only looking at the bottom part of the silo. This can also explain why the clogged experiment no longer has higher levels of disorder when the system is fully cropped, as seen in Figure 5.8, since we have since we have removed the corners from the interrogation region.

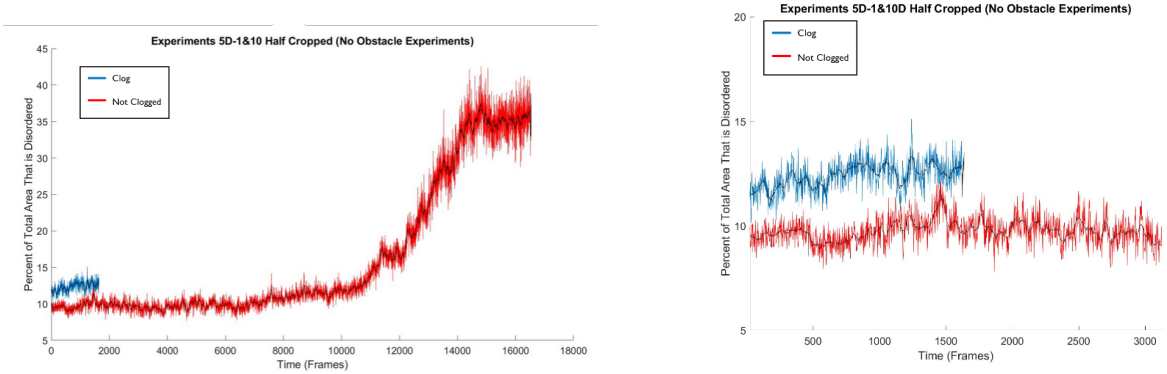

(a) (b)

Figure 5.7: Experiments with a 5D aperture, no obstacle, and half cropped. b) is a zoomed in version of a).

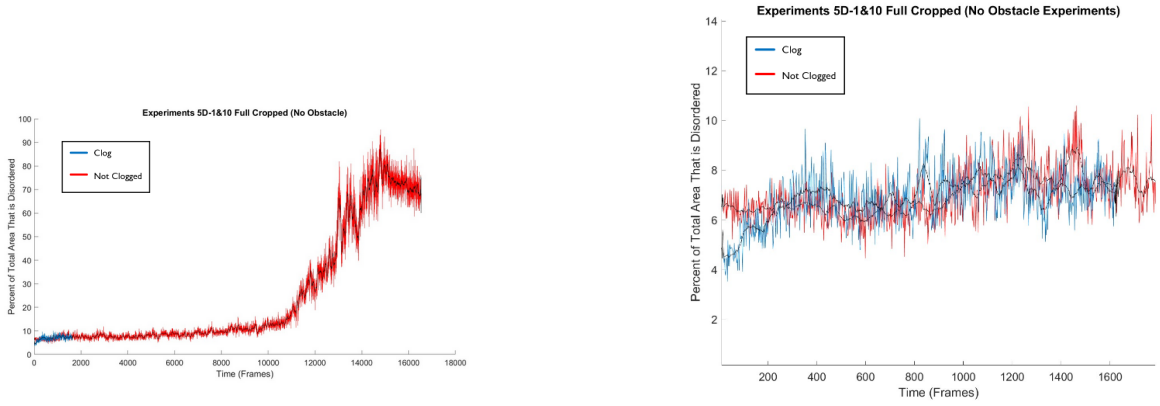

(a) (b)

Figure 5.8: Experiments with a 5D aperture, no obstacle, and full cropped. b) is a zoomed in version of a).

6 DISCUSSION AND CONCLUSIONS

6.1. Obstacles and Flow

When comparing the amount of disorder in the experiments with and without an obstacle, we can see a consistent overall higher level of disorder in the systems with obstacles. This could be due to two main reasons. First, due to the obstacle not being counted as a particle, we are getting rings of disordered particles around the obstacle. Second, as previously talked about in Section 3.4, obstacles increase the overall mobility and granular temperature in a system. This increase in particle movement in a system could be the reason for the higher amount of disorder in the systems with obstacles.

Another interesting aspect of the disorder graphs that changes between the obstacle and no obstacle experiments is the overall shape of the graphs. The experiments with the obstacle have a more pronounced downward slope prior to the sharp incline, while the experiment with the obstacle have a significantly less pronounced downward slope prior to the increase in disorder at the end. Both experiments have a sharp increase in disorder, and we believe this is due to the system running out of particles and therefore no longer being able to maintain larger groups of hexagonal packed particles. Difference in the shape of the graphs for the obstacle experiments could be indicative of the way obstacles change the flow of a system. To clearly understand what is causing the changes in the shape of the graph, more analysis will need to be done to properly compare experiments with and without obstacles, as well as the effect of different obstacles sizes, shapes, and placements on the graph shape.

6.2. Disordered Packing as an Indicator for Clogging

As discussed previously, increases in disorder in jamming systems have been shown to correspond to jamming transitions. The original goal of this research was to see if that metric of predicting jamming was applicable to systems that clog due to the similarities between those two behaviors. From the experiments we have analyzed, there is not a distinct enough difference in behavior between the experiments that clog and their non-clogging counterparts to say that disorder is indicative of clogging. This is inline with previous research in this field. Previous research indicates that there is likely no difference between a clog or non-clog with the same set-up, so it is reassuring that there is no indication in the levels of disorder as a system approaches a clog [36].

Due to the connection between overall higher disorder in systems with obstacles, there is a possible connection between higher disorder in a system and mobility or granular temperature. While more experimental analysis would be needed to fully confirm these ideas, the way we have been measuring disorder could be indicative of overall clogging probability in a system, in a similar way granular temperature can indicate systems that are less likely to clog. As stated in Section 3.4, while a majority of the experiments with a 4.5D sized aperture clogged, the set-ups with the lowest clogging probability were the same set-ups with the highest V_x standard deviation and V_{mag}. With the amount of data we currently have to compare, it seems that the overall levels of disorder in our systems could be indicating something similar to the average V_{mag} and V_x standard deviation discussed in Section 3.4. If this analysis is run on significantly more trials of an experimental set-up, upwards of 100 compared to the 5 of each trial we have, by chance there could be some

trials with significantly higher disorder which could be seen as a clearer indication of a system not clogging [44].

6.3. Further Work

With successful proof of concept, there are lots of ways to continue this work. The shielding analysis code used to get these results needs to be used on significantly more experiment trials with different obstacles, sizes, and locations. These can then be compared with each other and with the average V_{mag} and V_x standard deviation data to see if these trends continue. For this research, we did not compare the overall disorder in experiments with different obstacle sizes to see if there are differences in the overall disorder depending on the size and placement of the obstacle. If the conclusions from this research are correct, experiments with larger obstacles placed closer to the obstacle should have overall higher levels of disorder compared to other experimental set-ups. The analysis method that we developed could also be a starting point to track the movement of the crystalline clusters or disordered areas through a system. This is a particularly interesting avenue as it could help answer questions left from Cai *et al.*[36].

In addition to the main method we used of looking at grain boundaries and disorder, there are many other methods that have been used to gain a better understanding of jamming systems that could be used on clogging systems. Some of these methods have been discussed in this paper, including strings and χ_4. These methods of analysis were used briefly for this research, but neither ended up being the focus of our analysis. These methods could help predict clogging as they are able to predict jamming, or they could help us understand slightly different aspects of clogging systems.

LITERATURE CITED

[1] H. M. Jaeger, S. R. Nagel, and R. P. Behringer, "Granular solids, liquids, and gases", Reviews of Modern Physics **68**, 1259–1273 (1996).

[2] E. Weeks, "Soft jammed materials", in (Jan. 1, 2007), pp. 2–1.

[3] D. J. Jerolmack and K. E. Daniels, "Viewing earth's surface as a soft-matter landscape", Nature Reviews Physics **1**, Publisher: Nature Publishing Group, 716–730 (2019).

[4] K. Lu and Z. Cao, "New understanding on the principle of earthquake", International Journal of Modern Physics B **35**, Publisher: World Scientific Publishing Co., 2150013 (2021).

[5] Hopper and silo bulk discharge flow rate calculation, `https://powderprocess.net/Powder_Flow/Bulk_Discharge_Rate.html` (visited on 04/21/2025).

[6] J. Goodenow, R. Orr, and D. Ross, "Mathematical models of water clocks",

[7] H. O. Physics, Ancient greece: the water clock (clepsydra) of ktesibios, History Of Physics, `http://www.history-of-physics.com/2017/08/ancient-greece-water-clock-clepsydra-of_14.html` (visited on 03/01/2025).

[8] Hourglass PNG image with transparent background, pngimg.com, `https://pngimg.com/image/93125` (visited on 03/01/2025).

[9] C. Mankoc, A. Janda, R. Arévalo, J. M. Pastor, I. Zuriguel, A. Garcimartín, and D. Maza, "The flow rate of granular materials through an orifice", Granular Matter **9**, 407–414 (2007).

[10] M. A. Madrid, J. R. Darias, and L. A. Pugnaloni, "Forced flow of granular media: breakdown of the beverloo scaling", Europhysics Letters **123**, Publisher: EDP Sciences, IOP Publishing and Società Italiana di Fisica, 14004 (2018).

[11] W. A. Bevertoo, T. A. Lextcer, and J. van, "The flow of granular solids through orifices",

[12] R. P. Behringer, "Jamming in granular materials", Comptes Rendus. Physique **16**, 10–25 (2015).

[13] M. Van Hecke, "Jamming of soft particles: geometry, mechanics, scaling and isostaticity", Journal of Physics: Condensed Matter **22**, 033101 (2010).

[14] C. Radin, "Random close packing of granular matter", Journal of Statistical Physics **131**, 567–573 (2008).

[15] M. Dong, J. Reimann, R. K. Annabattula, and Y. Gan, "Morphological characterisation of 2d packing with bi-disperse particles", International Journal of Advances in Engineering Sciences and Applied Mathematics **13**, 89–97 (2021).

[16] D. Gollin, E. Bowman, and P. Shepley, "Granular temperature measurements of uniform granular flows",

[17] I. Zuriguel, D. R. Parisi, R. C. Hidalgo, C. Lozano, A. Janda, P. A. Gago, J. P. Peralta, L. M. Ferrer, L. A. Pugnaloni, E. Clément, D. Maza, I. Pagonabarraga, and A.

Garcimartín, "Clogging transition of many-particle systems flowing through bottlenecks", Scientific Reports **4**, Publisher: Nature Publishing Group, 7324 (2014).

[18] A. B. Harada, E. Thackray, and K. N. Nordstrom, "Silo flow and clogging in the presence of an obstacle", Physical Review Fluids **7**, Publisher: American Physical Society, 054301 (2022).

[19] E. G. Teich, K. L. Galloway, P. E. Arratia, and D. S. Bassett, "Crystalline shielding mitigates structural rearrangement and localizes memory in jammed systems under oscillatory shear", Science Advances **7**, Publisher: American Association for the Advancement of Science, eabe3392 (2021).

[20] H. Péter, A. Libál, C. Reichhardt, and C. J. O. Reichhardt, "Crossover from jamming to clogging behaviours in heterogeneous environments", Scientific Reports **8**, 10252 (2018).

[21] L. Berthier, "Dynamic heterogeneity in amorphous materials", Physics **4**, Publisher: American Physical Society, 42 (2011).

[22] L. Berthier and G. Biroli, "Theoretical perspective on the glass transition and amorphous materials", Reviews of Modern Physics **83**, Publisher: American Physical Society, 587–645 (2011).

[23] A. R. Abate and D. J. Durian, "Topological persistence and dynamical heterogeneities near jamming", Physical Review E **76**, Publisher: American Physical Society, 021306 (2007).

[24] A. S. Keys, A. R. Abate, S. C. Glotzer, and D. J. Durian, "Measurement of growing dynamical length scales and prediction of the jamming transition in a granular material", Nature Physics **3**, Publisher: Nature Publishing Group, 260–264 (2007).

[25] C. Dalle-Ferrier, C. Thibierge, C. Alba-Simionesco, L. Berthier, G. Biroli, J.-P. Bouchaud, F. Ladieu, D. L'Hôte, and G. Tarjus, "Spatial correlations in the dynamics of glassforming liquids: experimental determination of their temperature dependence", Physical Review E **76**, Publisher: American Physical Society, 041510 (2007).

[26] P. Zhang, J. J. Maldonis, Z. Liu, J. Schroers, and P. M. Voyles, "Spatially heterogeneous dynamics in a metallic glass forming liquid imaged by electron correlation microscopy", Nature Communications **9**, Publisher: Nature Publishing Group, 1129 (2018).

[27] A. Lefèvre, L. Berthier, and R. Stinchcombe, "Spatially heterogeneous dynamics in a model for granular compaction", Physical Review E **72**, Publisher: American Physical Society, 010301 (2005).

[28] A. Ferguson and B. Chakraborty, "Spatially heterogenous dynamics in dense, driven granular flows", EPL (Europhysics Letters) **78**, 28003 (2007).

[29] L. E. Silbert, "Temporally heterogeneous dynamics in granular flows", Physical Review Letters **94**, Publisher: American Physical Society, 098002 (2005).

[30] L. Li and J. E. Andrade, "Identifying spatial transitions in heterogenous granular flow", Granular Matter **22**, 52 (2020).

[31] H. Katsuragi, A. R. Abate, and D. J. Durian, “Jamming and growth of dynamical heterogeneities versus depth for granular heap flow”, Soft Matter **6**, 3023 (2010).

[32] A. R. Abate, “JAMMING IN THE GAS-FLUIDIZED BED”, PhD thesis (2006).

[33] C. Donati, J. F. Douglas, W. Kob, S. J. Plimpton, P. H. Poole, and S. C. Glotzer, “Stringlike cooperative motion in a supercooled liquid”, Physical Review Letters **80**, Publisher: American Physical Society, 2338–2341 (1998).

[34] G. Szamel and E. Flenner, “Four-point susceptibility of a glass-forming binary mixture: brownian dynamics”, Physical Review. E, Statistical, Nonlinear, and Soft Matter Physics **74**, 021507 (2006).

[35] D. Chandler, J. P. Garrahan, R. L. Jack, L. Maibaum, and A. C. Pan, “Lengthscale dependence of dynamic four-point susceptibilities in glass formers”, Physical Review E **74**, Publisher: American Physical Society, 051501 (2006).

[36] G. Cai, A. B. Harada, and K. Nordstrom, “Mesoscale metrics on approach to the clogging point”, Granular Matter **23**, 69 (2021).

[37] C. R. Berardi, K. Barros, J. F. Douglas, and W. Losert, “Direct observation of string-like collective motion in a two-dimensional driven granular fluid”, Physical Review E **81**, Publisher: American Physical Society, 041301 (2010).

[38] H. Zhang, D. J. Srolovitz, J. F. Douglas, and J. A. Warren, “Grain boundaries exhibit the dynamics of glass-forming liquids”, Proceedings of the National Academy of Sciences **106**, Publisher: Proceedings of the National Academy of Sciences, 7735–7740 (2009).

[39] J. C. Crocker and D. G. Grier, "Methods of digital video microscopy for colloidal studies", Journal of Colloid and Interface Science **179**, 298–310 (1996).

[40] R. Caitano, A. Garcimartín, and I. Zuriguel, "Anchoring effect of an obstacle in the silo unclogging process", Physical Review Letters **131**, Publisher: American Physical Society, 098201 (2023).

[41] K. Endo, K. A. Reddy, and H. Katsuragi, "Obstacle-shape effect in a two-dimensional granular silo flow field", Physical Review Fluids **2**, 094302 (2017).

[42] T. Andrei, 1.2: radial distribution function, Chemistry LibreTexts, (Jan. 17, 2021) https://chem.libretexts.org/Bookshelves/Biological_Chemistry/Concepts_in_Biophysical_Chemistry_(Tokmakoff)/01%3A_Water_and_Aqueous_Solutions/01%3A_Fluids/1.02%3A_Radial_Distribution_Function (visited on 05/08/2025).

[43] A. Brasiello, 18: radial distribution function of liquid argon. | download scientific diagram, ResearchGate, (Jan. 1, 2006) https://www.researchgate.net/figure/Radial-distribution-function-of-liquid-argon_fig17_228387451 (visited on 05/21/2025).

[44] C. M. Carlevaro, R. Kozlowski, and L. A. Pugnaloni, "Flow rate in 2d silo discharge of binary granular mixtures: the role of ordering in monosized systems", Frontiers in Soft Matter **4**, Publisher: Frontiers, 10.3389/frsfm.2024.1340744 (2024).

A APPENDICES

A.1. Shielding Code MATLAB Environment

```
 1 %prep stuff
 2 experiment = "tr_Z_5D_17D_15D_24p5DL_5"; %experiment title
 3 pathname = 'C:
\Users\nordstromlab\Desktop\Giselle\clustersave\
tr_Z_5D_17D_15D_24p5DL_5\';
 4 maxx=max(trAllFiltered(:,2));%MAX X
 5 maxy=max(trAllFiltered(:,1));%MAX y
 6 minx =min(trAllFiltered(:,2));%min x
 7 miny =min(trAllFiltered(:,1));%min y
 8 %set "box" for numPy output
 9 box = [maxx-minx, maxy,0,0,0,0]';
 10
 11 %python variables
 12 cluster_thresh = 9; %OG 3.2
 13 neighbors = 6; %OG 6
 14
 15 %shift tr with these maxes to have 0,0 in middle
 16 %% Big Loop of everything
 17 lastframe = max(trAllFiltered(:,3));
 18 % lastframe = 7001;
 19 figure() %NEW STUFF DELEAT IF DIDNT WORK
 20 for i = 1:2:lastframe
 21 %prepare tr for numpy (+1, 0,0 at middle)
 22 clear tracks positions
 23
 24 trAllFiltered = sortrows(trAllFiltered,[3,4]);
 25 track = trAllFiltered(trAllFiltered(:,3)==i,:);
 26 positions(:,1)=track(:,2)-maxx/2-minx/2;
 27 positions(:,2)=track(:,1)-maxy/2;
 28 positions(:,3) =0;
 29
 30
```

```
 31 %% Run Shielding Code from Python
 32 %NOTES FOR DEBUGGING PYTHON IN MATLAB
 33 % for jupyter file -> export as -> executable script (which is .py)
 34
 35 % pyenv("Version","/opt/anaconda3/envs/matlab/bin/python")
 %only need to do once? %MAC COMMAND
 36 % pyenv("Version","C:\Users\nordstromlab\AppData\Local\anaconda3
 \envs\matlab\python.exe") %WINDOWS COMMAND (needs .exe on the end)
 37 cluster_arrT = pyrunfile("C:\Users\nordstromlab\Desktop\
 calculate_shielding.py",
"testP",box=box,positions=positions, neighbors = neighbors,
cluster_thresh = cluster_thresh);
 38
 39
 40 %% python output crystal groups, do stuff with it in MATLAB
 41 cluster_arr = double((cluster_arrT))'+ 1;
 % +1 to swap back to MATLAB index starting at 1 from python start 0
 42
 43 % histogram(cluster_arr,'BinWidth',2)
 44
 45 [uv, ~, idx] = unique(cluster_arr); %find unique values
 46 n = accumarray(idx,1); %count how many times those values appear
 47
 48 threshold = 6;
 49 thresh_group = uv(n(:)>threshold,1);
 %reduce groups to above threshold
 50
 51 % not_thresh_group = uv(n(:)<threshold, 1);
 %number of particles that didn't pass the threshold (grain boundries)
 52
 53 [~,idxsort] = sort(n(n(:)>threshold),'descend');
 54 thresh_group = thresh_group(idxsort);
 55
 56
 57
 58 cm = colormap(turbo(length(thresh_group)));
 %set colormap to thresholded # groups
 59
```

```
60 %assign color for all particles
61 col = zeros(length(cluster_arr),3);
62 dotsize = zeros(length(cluster_arr),1);
63
64 [A,B] = ismember(cluster_arr, thresh_group);
%find if T/F in group: A= T/F, B = index of reduced color
65 col(A==1,:) = cm(B(A==1),:); %assign T color
66 % col(A==0),:) = [0,0,0]; %assign F color
67 % not necessary with preallocate 0;
leaving for clarity if you want to use [1,1,1] instead
68 dotsize(A==1,:) = 20; %assign T size
69 dotsize(A==0,:) = 2; %assign F size
70
71
72 scatter(positions(:,1), positions(:,2),dotsize,col,'Filled')
73 axis equal
74 axis tight
75 box on
76
77 cb = colorbar;
78 cb_chunk = 1/length(cm); %how large each chunk of color is
79 % %simple version
80 % cb.Ticks = cb_chunk/2:cb_chunk:1-cb_chunk/2;
%put ticks in the middle of each color segment
81 % cb.TickLabels = 1:1:length(cm);
82
83 %complex version by #
84 if length(cm) <= 20
85 cb.Ticks = cb_chunk/2:cb_chunk:1-cb_chunk/2;
%put ticks in the middle of each color segment
86 cb.TickLabels = 1:1:length(cm);
87 elseif length(cm) > 50
88 cbt = cb.Ticks;
89 set(cb,'TickLabels', num2str(round(cbt*length(cm))'))
90 elseif mod(length(cm),2) == 0 %20-50 even
91 cb.Ticks = 3*cb_chunk/2:2*cb_chunk:1;
92 cb.TickLabels = 2:2:length(cm);
93 else %20-50 and odd
```

```
 94 cb.Ticks = cb_chunk/2:2*cb_chunk:1-cb_chunk/2;
 %put ticks in the middle of each color segment
 95 cb.TickLabels = 1:2:length(cm);
 96 end
 97
 98 filename = strcat(pathname, "cluster_",experiment, "_",num2str(i));
 99 saveas(gcf,filename, 'tiff')
100
101
102 % histogram(cluster_arr(A),'BinWidth',2) %sanity figure
103 % xlim([0 40])
104 % saveas(gcf,strcat(filename, '_hist'), 'tiff')
105
106 % [col_uv, ~, col_idx] = unique(col);
107 % clust_max = max(col_idx);
108
109 %% plot of whole video
110 cluster_arrPositions = cat(2,cluster_arr,positions);
111
112
113 % %axis positions are based on positionss/scale from scatter plots
114 % cluster_arrPositions(cluster_arrPositions(:,2)>100,:)=[];
%kill those frames (x axis) FOR MORE FILTERING
115 % cluster_arrPositions(cluster_arrPositions(:,2)<-100,:)=[];
%kill those frames x axis) FOR MORE FILTERING
116 % % % %
117 % cluster_arrPositions(cluster_arrPositions(:,3)>0,:)=[];
%kill those frames (y axis) FOR MORE/HALF FILTERING switched from < to >
due to flow videos being flipped
118
119 [uvGB, ~, idxGB] = unique(cluster_arrPositions(:,1));
%find unique values
120 n = accumarray(idxGB,1); %count how many times those values appear
121 not_thresh_group = uvGB(n(:)<threshold, 1);
122
123 nparticle = size(cluster_arrPositions(:,1)==1,1);
%I think total number of particles in the frame
124 % nparticleYES = size (cluster_arr(A)==1,1);
```

```
% i think total number of particles that are in clusters
125 nparticleNO = size(not_thresh_group(:,1)==1,1);
126 % percent_cluster = (nparticleYES / nparticle) *100;
127 percent_grain(i,:) = (nparticleNO/nparticle)*100;
128
129
130
131
132
133 %%
134
135
136 end %for fr
137
138
139 PG=(percent_grain(1:2:lastframe));
140 smoothPG = smoothavg(percent_grain(1:2:lastframe),21);
141 plot(1:2:lastframe,percent_grain(1:2:lastframe,:),'-r')
142 hold on
143 plot(1:2:lastframe,smoothPG,'-black');
144 hold off
145 clustFilename = strcat(pathname, experiment, '_percentGrain');
146 saveas(gcf,clustFilename,'tiff')
147 saveas(gcf, clustFilename, 'fig')
148 DataFile = strcat(pathname, experiment, '_data');
149 save(DataFile,"PG","nparticleNO","nparticle","thresh_group",
"not_thresh_group")
150 %
151
152 % save(clustFilename);
153 % fileID = fopen([clustFilename],'w');
154 % fprintf(fileID,'\n max clust %d \n', clust_max);
155 % fclose(fileID);
```